Phosphorylation of the Light-Harvesting Complex II Isoform Lhcb2 Is Central to State Transitions[1][OPEN]

Paolo Longoni, Damien Douchi, Federica Cariti, Geoffrey Fucile, and Michel Goldschmidt-Clermont*

Department of Botany and Plant Biology (P.L., D.D., F.C., G.F., M.G.-C.) and iGE3, Institute of Genetics and Genomics of Geneva (M.G.-C.), University of Geneva, 1211 Geneva 4, Switzerland

ORCID IDs: 0000-0003-0587-7621 (P.L.); 0000-0002-6155-9153 (D.D.).

Light-harvesting complex II (LHCII) is a crucial component of the photosynthetic machinery, with central roles in light capture and acclimation to changing light. The association of an LHCII trimer with PSI in the PSI-LHCII supercomplex is strictly dependent on LHCII phosphorylation mediated by the kinase STATE TRANSITION7, and is directly related to the light acclimation process called state transitions. In Arabidopsis (*Arabidopsis thaliana*), the LHCII trimers contain isoforms that belong to three classes: Lhcb1, Lhcb2, and Lhcb3. Only Lhcb1 and Lhcb2 can be phosphorylated in the N-terminal region. Here, we present an improved Phos-tag-based method to determine the absolute extent of phosphorylation of Lhcb1 and Lhcb2. Both classes show very similar phosphorylation kinetics during state transition. Nevertheless, only Lhcb2 is extensively phosphorylated (>98%) in PSI-LHCII, whereas phosphorylated Lhcb1 is largely excluded from this supercomplex. Both isoforms are phosphorylated to different extents in other photosystem supercomplexes and in different domains of the thylakoid membranes. The data imply that, despite their high sequence similarity, differential phosphorylation of Lhcb1 and Lhcb2 plays contrasting roles in light acclimation of photosynthesis.

Light capture and its conversion to chemical energy occur in a set of transmembrane protein complexes of the thylakoid membrane. PSII, the cytochrome b_6f complex, and PSI drive photosynthetic electron flow and the creation of a proton gradient across the thylakoid membrane. ATP synthase couples the dissipation of this gradient to the synthesis of ATP. The light-harvesting antennae play an important role in collecting light and transferring energy to the photosystems. Light-Harvesting Complex I (LHCI) exclusively transfers light energy to PSI, with which it is tightly associated (Croce and van Amerongen, 2014). In contrast, LHCII, which is the most abundant complex of the thylakoid membrane, can transfer energy to PSI or PSII (Grieco et al., 2015). Light is highly variable in natural environments, and plants experience continuous changes in both the spectrum and intensity of light on

timescales as short as seconds. Changes in light quality may unbalance the activity of the two photosystems since their absorption spectra differ, whereas high light intensity can lead to overexcitation and induce photodamage. At low or moderate light intensities, the LHCII complex differentially associates with PSII or PSI, in a phosphorylation-dependent process known as state transitions, to rapidly respond to changes in the spectrum of light. In brief, under light quality that activates PSII more than PSI (e.g. blue light), LHCII is phosphorylated, and as a consequence, its binding to PSI is favored (state 2). Conversely, under light that preferentially excites PSI (enriched in far-red), this association can be reverted by dephosphorylation of the LHCII antenna, which favors its binding to PSII (state 1; Goldschmidt-Clermont and Bassi, 2015; Kim et al., 2015). A protein kinase, STATE TRANSITION7 (STN7), and a protein phosphatase, PROTEIN PHOSPHATASE1 (PPH1)/THYLAKOID-ASSOCIATED PHOSPHATASE38 (TAP38), are essential for the rapid phosphorylation and dephosphorylation of the LHCII antenna that regulates its differential association to PSI or PSII (Bellafiore et al., 2005; Pribil et al., 2010; Shapiguzov et al., 2010). Only a relatively small fraction of the LHCII antenna (<20%) is estimated to participate in state transitions in Arabidopsis (*Arabidopsis thaliana*; Allen, 1992). However, the process is conserved across the green eukaryotes and is relevant to plant fitness (Frenkel et al., 2007). Under high light, energy-dependent quenching of LHCII predominates, and furthermore, this antenna can uncouple from PSII (Wientjes et al., 2013b).

The differential association of photosystems, LHCII, and other components of the thylakoid membrane

gives rise to a set of supercomplexes that are central in ensuring photosynthetic efficiency and a rapid response to environmental cues (Caffarri et al., 2009; Duffy et al., 2013; Pietrzykowska et al., 2014; Fristedt et al., 2015). Fine tuning the dynamic assembly of these supercomplexes involves the association of antennae containing specific sets of Lhcb proteins. The major LHCII antenna comprises homo- and heterotrimers of Lhcb1 to Lhcb3 (Jackowski et al., 2001), whereas the minor LHCII isoforms (Lhcb4–Lhcb6) are monomeric (de Bianchi et al., 2008). Lhcb1 and Lhcb2 share a very similar primary structure and associated pigments (Formaggio et al., 2001; Zhang et al., 2008), whereas Lhcb3 appears to have slightly different features (Standfuss and Kühlbrandt, 2004). In Arabidopsis, five genes encode Lhcb1 isoforms, three genes encode Lhcb2 isoforms, and a single gene encodes Lhcb3. The principal discriminant between these classes is a short stretch of residues at the N-terminal end, which is of particular importance since it contains the Thr that is reversibly phosphorylated during light-acclimation processes (Goldschmidt-Clermont and Bassi, 2015). During evolution, land plants have maintained a major LHCII composed of different classes of Lhcb subunits. The phosphorylated N terminus of Lhcb2 was particularly well conserved (Alboresi et al., 2008; Zhang et al., 2008).

PSII-LHCII supercomplexes have been isolated from Arabidopsis with up to four LHCII trimers bound to a PSII dimer, as well as the three minor monomeric antennae (Lhcb4–Lhcb6; Caffarri et al., 2009; Kouřil et al., 2012). In the LHCII trimers of these supercomplexes, different classes of Lhcb subunits are distributed differently, suggesting a specific role in light acclimation for each of them (Damkjaer et al., 2009; Pietrzykowska et al., 2014). In the stably bound S trimer, Lhcb1 and Lhcb2 are more abundant, whereas the moderately bound M trimer contains mostly Lhcb1 and Lhcb3 (Galka et al., 2012). PSII supercomplexes isolated from spinach (Spinacia oleracea) showed the presence of an extra LHCII trimer (L trimer); therefore, it is possible that, in Arabidopsis, other trimers are associated with the PSII dimer in a more labile supercomplex that cannot be isolated (Boekema et al., 1999). A single LHCII trimer, containing Lhcb1 and Lhcb2, stably associates with PSI to constitute the PSI-LHCII supercomplex, whose formation is dependent on LHCII phosphorylation by STN7 in state 2 (Kouřil et al., 2005; Galka et al., 2012).

Previous reports have shown that the relative phosphorylation of Lhcb1 and Lhcb2 isoforms differs among thylakoid supercomplexes (Galka et al., 2012; Leoni et al., 2013). Here, we address the specific roles of Lhcb1 and Lhcb2 phosphorylation in photosynthetic acclimation. The improved protocol for SDS-PAGE in the presence of Phos-tag (Wako Chemicals) that we present allows quantification of the extent of phosphorylation for each class of antenna isoforms. We report that, in the PSI-LHCII supercomplex that is assembled in state 2, only the phosphorylated form of Lhcb2 is present,

whereas the phosphorylated form of Lhcb1 is excluded. In contrast, both Lhcb1 and Lhcb2 are phosphorylated to different levels in other supercomplexes. This quantitative information on the level of phosphorylation of Lhcb1 and Lhcb2 offers new insights into the specific roles of the two classes of LHCII isoforms in light acclimation and supercomplex formation.

RESULTS

An Improved Phos-tag PAGE Protocol Allows a Quantitative Measurement of Antenna Phosphorylation

Phos-tag, together with a chelated divalent cation such as Zn^{2+}, binds phosphate groups. Thus, using electrophoresis in polyacrylamide gels containing immobilized Phos-tag (Phos-tag PAGE), phosphorylated proteins can be resolved from their non-phosphorylated form because their migration is selectively retarded (Bekešová et al., 2015). Although the different phosphorylated forms are separated, the abundance of the phosphorylated forms relative to the nonphosphorylated protein remains difficult to quantify by immunoblotting. The main reason is that, since Phos-tag retards the phosphoprotein during electrophoresis, it also hampers its subsequent transfer to a membrane, leading to incomplete transfer of the phosphorylated form and, therefore, to an underestimation of phosphorylation. This problem can be partly alleviated by incubating the gel in EDTA-containing solution to strip Zn^{2+} prior to the transfer (Kinoshita et al., 2009). Here, we use an improved protocol with a two-layer resolving gel containing the Phos-tag ligand only in the upper layer. Phosphoproteins are retarded during their migration through the upper layer and then enter the lower layer, from which they can be transferred to a membrane without the interference of Phos-tag.

Using the two-layer Phos-tag PAGE protocol, phosphorylated Lhcb1 (P-Lhcb1) and P-Lhcb2 were resolved from the unphosphorylated forms (Fig. 1). The regulation of LHCII trimer binding to different photosystem supercomplexes involves phosphorylation of a single Thr residue at position 3 from the N terminus generated after removal of the transit peptide (Rochaix, 2014). Immunoblotting with phospho-specific antibodies against P-Lhcb1 or P-Lhcb2 confirmed that the top band represents the protein with the N-proximal Thr phosphorylation (Fig. 1; Leoni et al., 2013). The major LHCII isoforms constitute a peculiar substrate for immunodetection: the only portion suitable to raise antibodies for a specific Lhcb class is the N terminus of the mature polypeptide, since the remaining portion shares very high sequence similarity with other Lhcb isoforms as well as with other antenna proteins. Thus, the Lhcb1 antibodies probably fail to recognize Lhcb1.4 due to its N-terminal sequence, which differs from the other Lhcb1 variants. Moreover, the N-terminal peptide used as antigen to raise isoform-specific antisera against Lhcb1 and Lhcb2 contains the phosphorylation site at Thr-3. It appeared likely that the presence or absence of
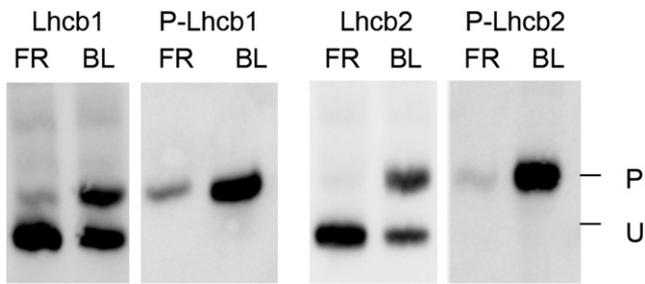
Figure 1. Two-layer Phos-tag PAGE resolves the phosphorylated and unphosphorylated forms of Lhcb1 and Lhcb2. Antisera against Lhcb1 or Lhcb2 recognize both bands, whereas phospho-specific antisera (P-Lhcb1 or P-Lhcb2) recognize only the slower migrating band, confirming that it represents the form that is phosphorylated at the N-proximal Thr. P and U indicate the phosphorylated and unphosphorylated forms, respectively. BL, Blue light; FR, far-red.

phosphorylation might influence recognition by the antisera. To assess this possible bias, the proteins transferred on the immunoblot membrane were subsequently treated with λ protein phosphatase. Indeed, with the antiserum against Lhcb2, phosphatase treatment of the membrane enhanced the signal of the phosphorylated form of the protein more than 2-fold (Supplemental Fig. S1). This treatment did not influence the signal for Lhcb1. After incubation with λ phosphatase, the signal obtained with phospho-specific antibodies against P-Lhcb1 or P-Lhcb2 became undetectable, showing that dephosphorylation of these proteins on the membrane was essentially complete (Supplemental Fig. S1). The phosphatase treatment of the membrane blot was therefore included in our improved protocol, which was used in all further experiments.

To determine the phosphorylation levels of Lhcb1 and Lhcb2, it is important to determine whether the respective antibodies are specific. This was previously shown in an analysis of antisense lines deficient in Lhcb1 or Lhcb2 (Pietrzykowska et al., 2014). The lack of cross reactivity was further confirmed using recombinant proteins expressed in *Escherichia coli* (Supplemental Fig. S2). To obtain quantitative data from immunoblotting, it is necessary to determine whether the signal is proportional to the amount of protein and in what range. Using different amounts of protein extracts with different levels of protein phosphorylation, there was a linear correlation between the signal obtained with the Lhcb1 or Lhcb2 antisera and the amount of total protein up to at least 5 μg with our protocol (Supplemental Fig. S3).

The two-layer Phos-tag PAGE protocol offers better transfer of the proteins from the Phos-tag-free part of the resolving gel to the membrane and, therefore, a reliable quantification of phosphorylation. This was confirmed for Lhcb1 and Lhcb2 as follows (Supplemental Fig. S4). Samples with widely different extents of phosphorylation were subjected to two-layer Phos-tag PAGE and immunoblotting. For each sample, the sum of the signals of the phosphorylated and nonphosphorylated forms was normalized to the signal of actin, the loading control.

This normalized sum remained nearly constant over the whole range of phosphorylation levels, indicating that there was no significant bias in the transfer of the phosphorylated form. If the phosphorylated form had been inefficiently transferred, a decrease of this sum with increasing phosphorylation would have been expected.

In summary, three control experiments validate the improved protocol for quantification of the extent of phosphorylation of Lhcb1 or Lhcb2: (1) the retarded band corresponds to the phosphorylated form, (2) there is a linear correlation of the signal with the amount of protein loaded, and (3) the sum of the signals of the phosphorylated and nonphosphorylated forms is nearly constant over a wide range of phosphorylation levels.

Lhcb1 and Lhcb2 Have Different Phosphorylation Levels

Although it is known that both Lhcb1 and Lhcb2 are phosphorylated, principally by the STN7 kinase, the extent of this phosphorylation for each class of LHCII antenna subunits was not known (Leoni et al., 2013). In 6-week-old plants exposed to low-intensity white light (70 μmol s^{-1} m^{-2}), the phosphorylation level of the two LHCII subunits was remarkably different (Fig. 2). Only a small fraction of Lhcb1 was phosphorylated (13% $\pm$
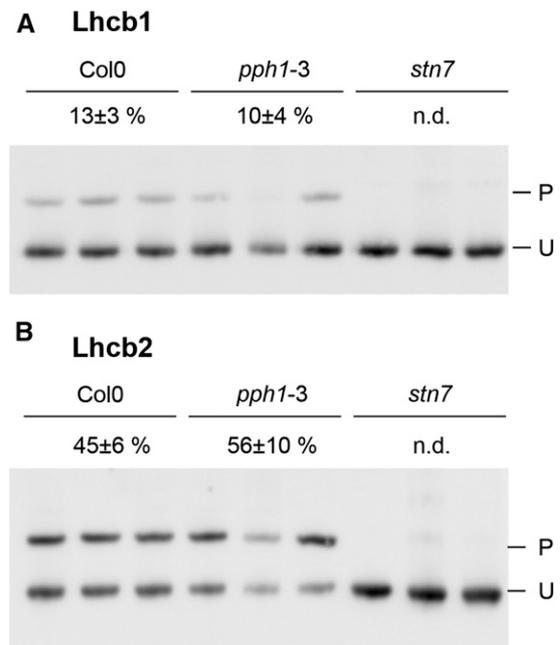

Figure 2. Lhcb phosphorylation in white light. Total protein from mature leaves of 6-week-old plants was subjected to two-layer Phos-tag PAGE. Three biological replicates are shown for each genotype. Wild-type Col0 (ecotype Columbia 0) plants are compared with the phosphatase mutant *pph1-3* and the kinase mutant *stn7*. The measured level of phosphorylation is indicated for each genotype above the immunoblots with the SD ($n = 5$; n.d., <1% of phosphorylation). P and U indicate the phosphorylated and unphosphorylated forms, respectively. A, Immunodetection of Lhcb1. B, Immunodetection of Lhcb2.
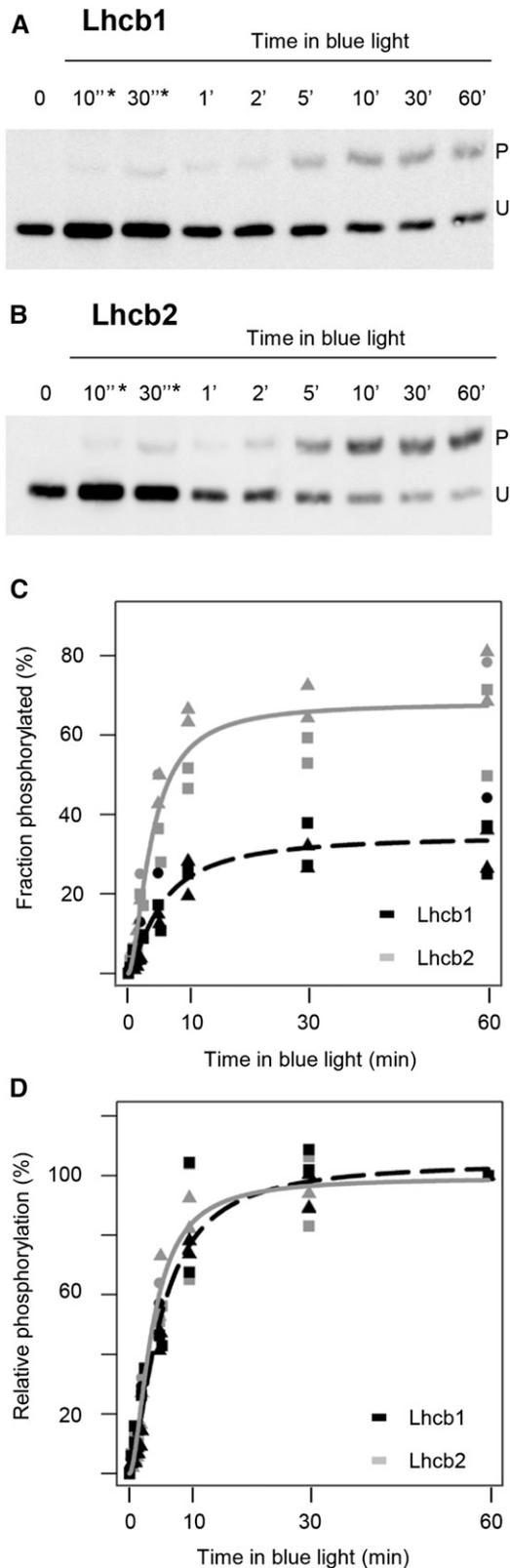
A **Lhcb1**

B **Lhcb2**

C

D

Figure 3. Phosphorylation kinetics upon a switch from far-red to blue light. Total protein was extracted from 15-d-old seedlings (three per time point) that were exposed to far-red light for 1 h and then switched to blue light. The level of phosphorylation was determined at different

3%), whereas Lhcb2 was more extensively phosphorylated (45% ± 6%; $n = 5$). To verify the effect of the lack of STN7, the major kinase acting on the antenna proteins, and of PPH1/TAP38, the main counteracting phosphatase, mutants for either protein were compared in terms of total phosphorylation level (Bellafiore et al., 2005; Shapiguzov et al., 2010). Whereas in the *stn7* kinase mutant, phosphorylation of Lhcb1 and Lhcb2 was reduced below the detection level, in the *pph1/tap38* phosphatase mutant, the fraction of P-Lhcb1 showed no difference compared with the wild-type value, and a slight increase in the Lhcb2 phosphorylation level was not statistically significant ($P > 0.10$; Fig. 2).

To increase antenna phosphorylation, mature leaves of adult plants were first subjected to 60 min of far-red light to favor PSI (state 1), followed by 60 min of blue light to preferentially excite PSII (state 2). The phosphorylated fraction of Lhcb1 increased to 31% ± 4%, whereas the phosphorylated portion of Lhcb2 was 54% ± 4% ($n = 4$; Supplemental Fig. S5). The same light regime applied to 15-d-old seedlings revealed a very similar phosphorylation trend (Fig. 3). The final phosphorylation level was not different from that observed in adult leaves for Lhcb1 (34% ± 8%), whereas it was even higher for Lhcb2 (69% ± 12%; $P < 0.05$; $n = 5$). It was previously reported that, in different plant species, including Arabidopsis, the kinetics of phosphorylation in a transition from state 1 to state 2 were faster for Lhcb2 compared with Lhcb1 (Jansson et al., 1990; Leoni et al., 2013). Here, the phosphorylation kinetics of the two subunits were measured during the shift from far-red to blue light in Arabidopsis 15-d-old seedlings (Fig. 3). The two antenna isoforms did not show a large difference in their relative phosphorylation kinetics, but differed in the final level of phosphorylation, with Lhcb2 more extensively phosphorylated than Lhcb1 (Fig. 3). Similar phosphorylation dynamics were observed in 6-week-old plants, even though the final level of phosphorylation was lower, as described above (Supplemental Fig. S5).

Phosphorylation of Antenna Isoforms in Different Supercomplexes

The phosphorylation of Lhcb1 and Lhcb2 in PSI and PSII supercomplexes was investigated using two-dimensional gel electrophoresis. Blue native (BN)-PAGE allows the separation of the main supercomplexes containing PSI or PSII associated with LHCII trimers.

times after the switch (time 0) to blue light. A, Immunodetection of Lhcb1. B, Immunodetection of Lhcb2. C, Phosphorylation levels for Lhcb1 (dotted black line) and Lhcb2 (plain gray lines) of five samples, such as those presented in A and B, are plotted as a function of time. The lines represent a sigmoidal fit of the data. Triangles, squares, and circles represent distinct biological replicates of the experiment. D, The same data as in C are normalized to the final phosphorylation level (phosphorylation at $t = 3,600$ s equals 100%). P and U indicate the phosphorylated and unphosphorylated forms, respectively.

Using different detergents, specifically digitonin or β-dodecylmaltoside (β-DM), it is possible to solubilize different fractions of the thylakoid membranes and thus to resolve a different set of supercomplexes (Järvi et al., 2011; Grieco et al., 2015). Digitonin releases the complexes from stromal lamellae and grana margins where most of PSI localizes, whereas β-DM also solubilizes the complexes in grana cores containing mostly PSII. The lanes obtained after BN-PAGE were used in a second dimension using two-layer Phos-tag PAGE (two-dimensional [2D] electrophoresis) to determine the degree of phosphorylation of the antenna isoforms in the different supercomplexes. More extensive phosphorylation of both Lhcb1 and Lhcb2 was observed in the supercomplexes solubilized after digitonin treatment compared with those obtained after β-DM treatment (Fig. 4). In the digitonin extract, Lhcb2 appeared more phosphorylated than Lhcb1 in all of the supercomplexes (higher P-to-U ratio in the 2D gel). Remarkably, Lhcb2 was phosphorylated to a very high extent when associated with the PSI-LHCII supercomplex, which is assembled upon antenna phosphorylation by STN7 in state 2. On the contrary, after β-DM solubilization, the supercomplexes from the grana cores, mostly containing PSII-LHCII, showed little LHCII phosphorylation, whereas most of the phosphorylated antenna was present in the free trimers (Fig. 4). To determine whether increased phosphorylation of the LHCII trimers would change the pattern of phosphorylation in the supercomplexes that can be recovered, thylakoids were prepared from *pph1-3* plants lacking the LHCII phosphatase, after a light shift from far-red to blue. For the supercomplexes extracted with digitonin, the phosphorylation pattern obtained after 2D gel electrophoresis did not noticeably change (Fig. 4). However, a difference was apparent for the grana core supercomplexes extracted with β-DM. In the *pph1-3* mutant, Lhcb2 phosphorylation increased in the PSII-LHCII supercomplexes with a clear trend: smaller complexes contained more extensively phosphorylated Lhcb2 than larger ones.

The differing abundance of Lhcb1 and Lhcb2 in the digitonin-extracted supercomplexes hinders the estimation of their respective phosphorylation levels by 2D electrophoresis. Furthermore, the shape of the spots leads to saturation of strong signals and a reduced range of linearity for the immunoblot assay. To confirm the observations and obtain quantitative estimates of the phosphorylation status of Lhcb1 and Lhcb2 in different supercomplexes, each band was cut after BN-PAGE of a
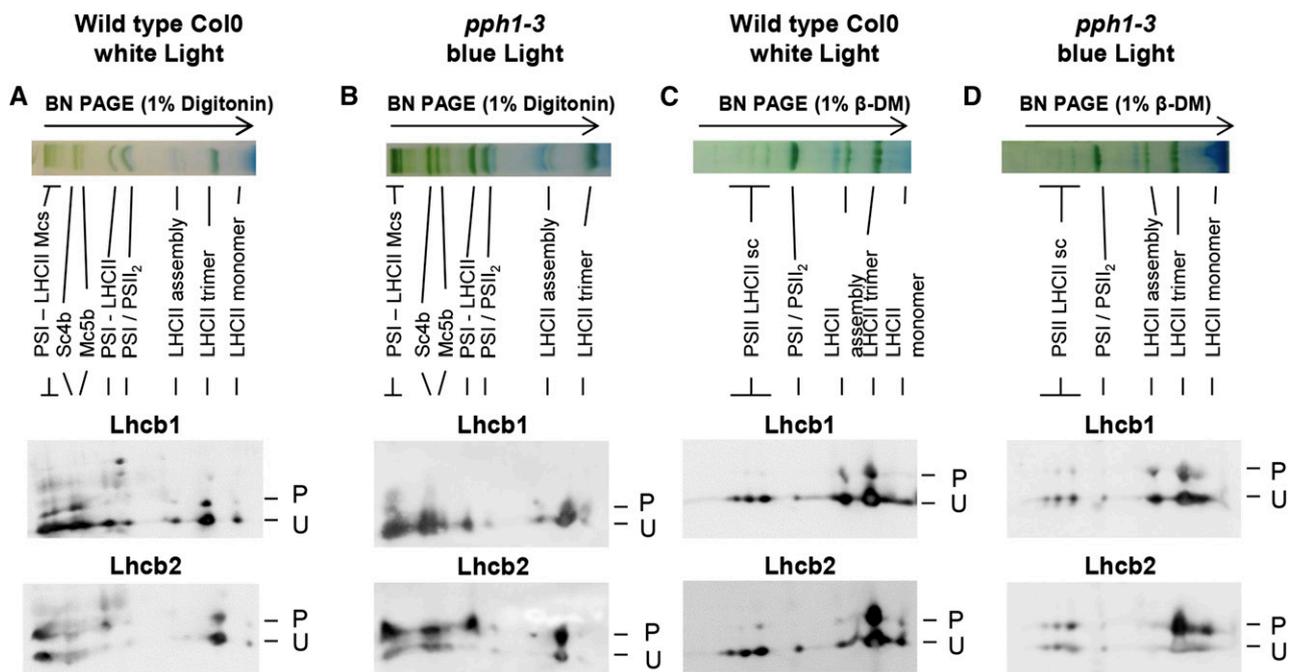

Figure 4. Lhcb1 and Lhcb2 phosphorylation in different supercomplexes. Wild-type Col0 (ecotype Columbia 0) plants were grown under white light (70 μmol sec^{-1} m^{-2}) and harvested 4 h after the onset of light. Thylakoid membranes were solubilized and subjected to BN-PAGE in the first dimension (top). The lanes were then subjected to a second dimension of two-layer Phos-tag PAGE and immunoblotting to reveal the phosphorylation of Lhcb1 and Lhcb2 (P, phosphorylated; U, unphosphorylated). A, Col0 wild-type plants were grown in white light. Thylakoid membranes were solubilized with digitonin. B, Mutant *pph1-3* plants were treated with far-red light (1 h) and then blue light (30 min) to increase antenna phosphorylation. Thylakoid membranes were solubilized with digitonin. C, Col0 plants were grown in white light as in A, and thylakoid membranes were solubilized with β-DM. D, Mutant *pph1-3* were treated as in B, and thylakoid membranes were solubilized with β-DM. The bands are labeled as described by Järvi et al. (2011): Mcs, megacomplexes; Sc4b, supercomplex 4b; Mc5b, megacomplex 5b; PSI-LHCII, STN7-dependent PSI-LHCI-LHCII supercomplex; PSI/PSII$_2$, comigrating PSI-LHCI and PSII dimer; LHCII assembly, LHCII complex containing an LHCII trimer associated with monomeric Lhcbs (mainly Lhcb4 and Lhcb6); and PSII LHCII sc, PSII dimer-LHCII supercomplexes.

digitonin extract and ground in SDS buffer, and the supernatant was then subjected to two-layer Phos-tag PAGE (Fig. 5). As suggested by the results of 2D gel electrophoresis, the PSI-LHCII supercomplex showed a unique phosphorylation pattern for the two classes of major LHCII isoforms. Lhcb2 was almost completely phosphorylated (over 98% in phosphorylated form), whereas Lhcb1 was essentially unphosphorylated (<1%; Supplemental Fig. S6). This is in agreement with the results in Fig. 4, where in the PSI-LHCII complex Lhcb2 was also strongly phosphorylated, whereas P-Lhcb1 was barely detectable compared with the strong and apparently saturated signal of its unphosphorylated form. It should be noted that the completely different patterns of phosphorylation confirm that the two antibodies are specific for their respective targets and do not show significant cross reactivity. Bands containing the PSII-LHCII supercomplexes extracted with β-DM from grana cores were also analyzed individually for antenna phosphorylation (Supplemental Fig. S7). This confirmed the observations from the 2D gels showing that Lhcb2 is more phosphorylated in the smaller PSII-LHCII supercomplex containing only one LHCII trimer than in the larger supercomplex containing two trimers.

It is important to note that this specific differential phosphorylation was unique to the PSI-LHCII supercomplex, since both Lhcb1 and Lhcb2 were present in partially phosphorylated form in other supercomplex-containing bands, with Lhcb2 generally more phosphorylated than Lhcb1 (Fig. 5). A relatively high level of Lhcb1 and Lhcb2 phosphorylation was observed in the Sc4b band and in the Mc5b band. Both were described to contain PSI, PSII, and LHCII, but fluorescence lifetime analysis indicated that PSII may not be functionally connected to PSI in these bands (Järvi et al., 2011; Yokono et al., 2015).

DISCUSSION

Phosphorylation Kinetics of Lhcb1 and Lhcb2

State transitions provide a rapid acclimatory response to changes in light quality and operate in the time range of a few minutes. Because of the different roles of Lhcb1 and Lhcb2 in the state transition supercomplex, it was of interest to examine the kinetics of their phosphorylation, which in both cases is dependent on the protein kinase STN7. It was previously reported that Lhcb2 is phosphorylated at a faster rate than Lhcb1 in Arabidopsis (Larsson et al., 1987; Leoni et al., 2013). However, when relative rates were compared in our work using two-layer Phos-tag PAGE, Lhcb1 and Lhcb2 were phosphorylated with very similar kinetics (Fig. 3). A possible reason for the discrepancy might be the light conditions used. In our study, state 1 was induced with far-red light only and state 2 by shifting to blue light, whereas in the previous work, far-red was added to a red-light background. It is possible that our conditions led to a more complete antenna dephosphorylation in state 1. The availability of the Lhcbs as substrates for the kinase may change under different light conditions (Zer et al., 2003; Kirchhoff, 2014). Furthermore, Lhcb2 is less abundant than Lhcb1. Thus, its higher phosphorylation level compared with Lhcb1 and its similar phosphorylation kinetics suggest that Lhcb2 is preferentially phosphorylated and appears to be a better substrate for the kinase(s) in terms of accessibility or recognition.

Antenna Phosphorylation in the PSI-LHCII State Transition Supercomplex

Some caution should be used in interpreting the phosphorylation of photosynthetic supercomplexes solubilized by detergent treatment of thylakoid membranes
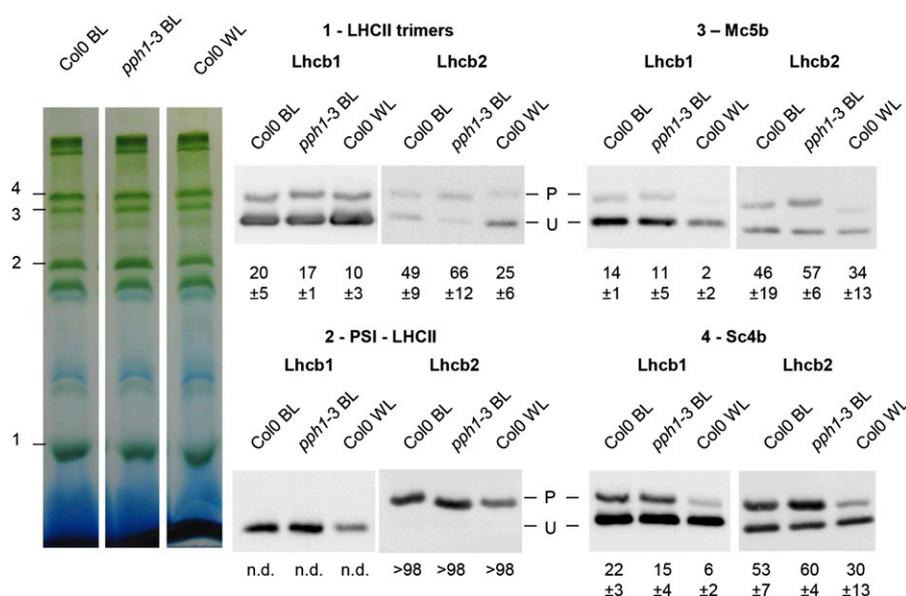

Figure 5. Quantification of Lhcb1 and Lhcb2 phosphorylation in supercomplexes. Wild-type Col0 (ecotype Columbia 0) and mutant pph1-3 plants were treated for 1 h with far-red light and then exposed to blue light for 30 min (BL). Wild-type Col0 were also grown under white light (70 μmol sec^{-1} m^{-2}) and harvested 4 h after the onset of light (WL). Thylakoid membrane complexes extracted with digitonin were subjected to BN-PAGE. Individual bands were cut as indicated on the left (1–4) and separately analyzed by two-layer Phos-tag PAGE and immunoblotting. The measured percentage of phosphorylation is indicated below each lane with its SD (n = 3). n.d., <1% phosphorylation.

and isolated by BN-PAGE. Several interrelated effects should be considered, including the role of phosphorylation in the regulated assembly of the complexes and in their stability in vivo, as well as the effect of phosphorylation on the lability of the complexes in vitro upon detergent extraction. Indeed, after BN-PAGE, a large proportion of LHCII is in the form of free trimers, which are most likely loosely bound in supercomplexes in vivo (Caffarri et al., 2009; Järvi et al., 2011; Pagliano et al., 2014; Grieco et al., 2015). Furthermore, PSII supercomplexes in the grana core may not be accessible to phosphorylation for steric reasons, because the tight appression of the membranes could hinder the access of the corresponding protein kinases (Zer et al., 2003; Kirchhoff, 2014).

The PSI-LHCII complex assembles in state 2 and involves the binding of a mobile trimer, which contains Lhcb1 and Lhcb2 (Galka et al., 2012), to the PSI complex. This association depends on the kinase STN7. An analysis of Arabidopsis knock-down lines lacking Lhcb1 or Lhcb2 previously suggested that the two isoforms play complementary roles in state transitions. Lhcb1 could largely replace Lhcb2 in the lines lacking Lhcb2. However these Lhcb2 knock-down mutants could not assemble the PSI-LHCII supercomplex or undergo state transitions (Pietrzykowska et al., 2014). Using phospho-specific antisera, it was also observed that PSI-LHCII is enriched in P-Lhcb2 but lacks P-Lhcb1 (Leoni et al., 2013). Although such antibodies could reveal relative differences in phosphorylation under different conditions or in different complexes, our two-layer Phos-tag PAGE method now allows a quantitative assessment of the absolute extent of phosphorylation.

We observed that, in the PSI-LHCII supercomplex, Lhcb2 is in fact almost entirely phosphorylated (>98%), whereas in contrast, Lhcb1 is not phosphorylated to measurable levels (<1%; Fig. 5; Supplemental Fig. S6). This implies that phosphorylation of Lhcb2 is key to the formation of PSI-LHCII. For state transitions, the reversible allocation of LHCII to the photosystems has been interpreted as a change in the relative affinity of the mobile LHCII trimer for PSI versus PSII (Haldrup et al., 2001). From this perspective, the formation or stability of the PSI-LHCII thus appears to depend on the phosphorylation of Lhcb2 and the lack of phosphorylation of Lhcb1. However, it cannot be excluded that PSI-LHCII complexes with both isoforms phosphorylated could assemble in vivo, but would be lost upon detergent solubilization and BN-PAGE because of a low stability.

It is also striking that the phosphorylated form of Lhcb1 is largely excluded from the PSI-LHCII supercomplex (Fig. 4), even though the presence of Lhcb1 appears to be crucial, since in knock-down lines lacking this isoform the supercomplex does not form (Pietrzykowska et al., 2014). The lack of Lhcb1 phosphorylation in PSI-LHCII could seem somewhat paradoxical, since STN7-dependent phosphorylation of both Lhcb1 and Lhcb2 is observed in conditions that favor a transition from state 1 to state 2 (Fig. 2; Leoni et al., 2013). An extreme view might be that phosphorylation of Lhcb2 is central, and that phosphorylation of Lhcb1 is a collateral effect, with

no specific function, due to the imperfect substrate specificity of the kinase(s) and phosphatase(s). However, it is also possible, and perhaps more likely, that phosphorylation of Lhcb1 is important in the regulation of other supercomplexes and/or of their localization in different domains of the thylakoid network.

Antenna Phosphorylation in the PSII-LHCII Supercomplexes

In the PSII-LHCII supercomplexes solubilized with β-DM from grana membranes, the phosphorylation of Lhcb1 and Lhcb2 is low. However, after a far-red to blue shift that induces high levels of phosphorylation, there is a clear difference in Lhcb2 phosphorylation
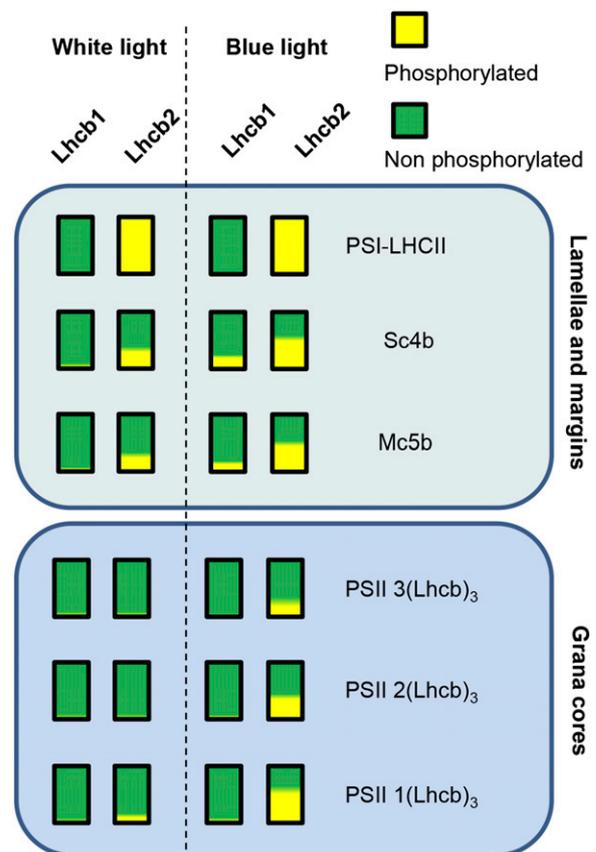

Figure 6. Lhcb1 and Lhcb2 phosphorylation in different supercomplexes. The extent of phosphorylation of Lhcb1 and Lhcb2 is depicted for the supercomplexes present in the stromal lamellae and grana margins (top box, digitonin extraction) and those present in the grana cores (bottom box, β-DM extraction). In each bar, yellow represents the proportion of P-Lhcb1 or P-Lhcb2, and green, the unphosphorylated fraction. Plants grown under white light (left of the dotted line) are compared with plants shifted to blue light after a far-red treatment to increase overall antenna phosphorylation (right of the dotted line). The complexes are labeled on the right (Järvi et al., 2011): PSI-LHCII, STN7-dependent PSI-LHCI-LHCII supercomplex; PSII-3(Lhcb)$_3$, PSII-LHCII supercomplex containing 3 LHCII trimers; PSII 3(Lhcb)$_2$, PSII-LHCII supercomplex containing 2 LHCII trimers; and PSII-1(Lhcb)$_3$, PSII-LHCII supercomplex containing 1 LHCII trimer.

between complexes of different sizes (Fig. 4; Supplemental Fig. S7). Phosphorylation of Lhcb2 is higher in complexes containing only one LHCII trimer, and gradually lower in complexes containing two or three trimers (Fig. 6). This could suggest that PSII-LHCII supercomplexes with high levels of LHCII trimer phosphorylation are less stable in vivo, or labile during extraction. An alternate possibility is that, in the smaller PSII-LHCII complexes, Lhcb2 is more accessible to the kinase, whereas in contrast, it is more deeply buried in the larger complexes. The latter hypothesis would fit with the previous observation that Lhcb2 is more abundant in the trimer (named S) most closely associated with the PSII core (Galka et al., 2012). However, Lhcb1 is more phosphorylated in large PSII-rich supercomplexes solubilized with digitonin from stromal lamellae and grana margins, whereas its level of phosphorylation in PSII-LHCII supercomplexes extracted with β-DM from grana cores is comparatively low (Fig. 6; Yokono et al., 2015). These observations suggest that Lhcb phosphorylation may contribute to the movement of the PSII-LHCII supercomplexes from grana cores toward less-stacked domains of the thylakoid membrane, grana margins, and stromal lamellae. This hypothesis is consistent with the recent proposal that phosphorylation of both the LHCII antenna and the PSII core assists the migration of PSII-LHCII out of grana (Mekala et al., 2015). The phosphorylation patterns of Lhcb1 and Lhcb2 may be rationalized by considering that, in low levels of white light, energy capture should be maximized by ensuring that all LHCII trimers are associated with photosystems. This would require a higher degree of Lhcb2 phosphorylation in the stromal lamellae and grana margins to promote binding of LHCII to PSI, and a lower level of Lhcb1 and Lhcb2 phosphorylation in the grana cores to avoid interference with the supramolecular organization of PSII-LHCII supercomplexes (Wientjes et al., 2013a). Under blue light and the ensuing transition toward state 2, a higher degree of Lhcb2 phosphorylation would increase the formation of the PSI-LHCII state transition complex in the grana margins, and would possibly favor the dissociation of the higher-order PSII-LHCII supercomplexes in the grana cores (Dietzel et al., 2011).

In conclusion, the optimized Phos-tag system presented in this work allows a detailed analysis of the phosphorylation of the proteins of interest, and allows a better understanding of the role and kinetics of protein phosphorylation. Finally, it should be emphasized that the contrasting phosphorylation of Lhcb1 and Lhcb2 in different photosynthetic supercomplexes implies that, in examining the physiology of light acclimation, it may be misleading to consider LHCII phosphorylation in bulk, and it is rather the phosphorylation of specific isoforms that should be taken into account.

MATERIALS AND METHODS

Plant Material and Light Conditions

Arabidopsis (*Arabidopsis thaliana*) ecotype Columbia 0 (hereafter Arabidopsis) plants were grown for 40 d at 22°C and 65% relative humidity under white light (70 μmol sec^{-1} m^{-2}) with 8 h of daylight. The light treatments were initiated 4 h after the beginning of the light period. Fifteen-day-old plantlets were grown at 22°C under white light (70 μmol sec^{-1} m^{-2}) with 16 h of daylight in a growth chamber (Percival CU36L5) on Murashige and Skoog agar plates supplemented with 1% (w/v) Suc. The mutant lines of PPH1/TAP38 and STN7 were previously described as *pph1-3* (Shapiguzov et al., 2010) and *stn7* (Bellafiore et al., 2005). For far-red and blue light treatment, the plants were placed under light-emitting diode panels (L735 and L470; Epitex).

Two-Layer Phos-tag PAGE

Total protein extract from seedlings or leaves was prepared as previously described (Samol et al., 2012). The total protein concentration was measured with bicinchoninic acid solution (Sigma-Aldrich) following the manufacturer's instructions. All chemicals were bought from Applichem-Panreac unless otherwise stated. The gel was prepared as follows: heavy resolving-gel solution: 357 mM Bis-Tris (pH 6.8; Roth), 30% (w/v) glycerol, 9% (w/v) acrylamide/ bis-acrylamide 37.5:1, 0.05% (v/v) *N,N,N',N'*-tetramethylethylenediamine (TEMED), 0.025% (w/v) ammonium persulfate (APS); light resolving-gel solution: 357 mM Bis-Tris (pH 6.8), 8% (w/v) acrylamide/bis-acrylamide 37.5:1, 60 μM Phos-tag (Wako Chemicals), 0.05% (v/v) TEMED, 0.05% (v/v) APS, 0.01% (w/v) Coomassie Brilliant Blue G-250 (Bio-Rad); stacking-gel solution: 357 mM Bis-Tris (pH 6.8), 4% (w/v) acrylamide/bis-acrylamide 37.5:1, 0.1% (v/v) TEMED, 0.05% (w/v) APS.

Three volumes of the heavy solution were poured between the gel plates, followed by 1 volume of the light solution. The two solutions were partially mixed with a nylon membrane to smooth the interface between the two layers. After the two-layer resolving gel polymerized, the stacking gel was cast. Samples were prepared in lithium dodecyl sulfate (LDS) loading buffer (10% [w/v] glycerol, 244 mM Tris HCl [pH 8.5], 2% [w/v] LDS, 0.33 mM Coomassie Brilliant Blue G-250, 100 mM dithiothreitol [DTT]) and heated for 5 min at 70°C before loading. Five micrograms of total protein sample was loaded per well. The PAGE was performed with freshly prepared running buffer (61 mM Tris, 50 mM MOPS, 0.1% [w/v] SDS, and 5 mM sodium bisulfite).

The gel was transferred overnight (16 h) onto a nitrocellulose membrane in a tank containing transfer buffer (500 mM Bicine [Sigma-Aldrich], 500 mM Bis-Tris, 20 mM EDTA, 10% [v/v] methanol, 5 mM sodium bisulfite [pH 7.2]). After staining with amido black (0.1% [w/v] amido black 10B in 30% [v/v] methanol, 10% [v/v] acetic acid), the membrane was treated with blocking buffer (3% [w/v] bovine serum albumin, 1× Tris-buffered saline [50 mM Tris-Cl, pH 7.5; 150 mM NaCl], 0.1% [v/v] Triton X-100) for 40 min with agitation. For dephosphorylation, the membrane was incubated in blocking buffer with 400 U mL^{-1} of λ protein phosphatase (New England BioLabs), 2 mM DTT, and 2 mM MnCl$_2$ for 4 h at room temperature. The membrane was washed twice with phosphate-buffered saline and deionized water before incubation with the primary antibody. For immunodetection, the Lhcb1 (AS09 522), Lhcb2 (AS01 003), P-Lhcb1 (AS13 2704), and P-Lhcb2 (AS13 2705) antibodies were from Agrisera, and the actin antibody (A0480) was from Sigma-Aldrich. After incubation with the secondary antibody (Promega) and enhanced chemiluminescence reagent, the chemiluminescence was detected using an LAS-4000 Mini cooled CCD camera (GE Healthcare Life Sciences). Band intensity was measured with ImageQuant (GE Healthcare Life Sciences) and ImageJ (National Institutes of Health) softwares.

Isolation of Thylakoid Membranes

Thylakoid membranes from 40-d-old Arabidopsis plants were isolated as previously described (Arnold et al., 2014). Detergent solubilization was performed with 1% (w/v) digitonin (Sigma-Aldrich) or 1% (w/v) β-DM (Calbiochem) as previously described (Järvi et al., 2011). Native gels for supercomplex separation were prepared as described (Schägger and von Jagow, 1991) using an acrylamide:bis-acrylamide ratio of 37.5:1, an acrylamide gradient of 3.5% to 12.5% (w/v) in the resolving gel, and an acrylamide concentration of 3% (w/v) in the stacking gel. The second dimension of 2D PAGE was performed as previously described (Järvi et al., 2011). Excised bands were ground with a pestle in Laemmli buffer (138 mM Tris-HCl [pH 6.8], 6 M urea, 22.2% [w/v] glycerol, 4.3% [w/v] SDS, and 5% [v/v] 2-mercaptoethanol), incubated for 1 h at 70°C, and then centrifuged in a microfuge. The supernatant was diluted 1 to 1 with 2× LDS loading buffer (20% [w/v] glycerol, 500 mM Tris-HCl [pH 8.5], 4% [w/v] LDS, 0.66 mM Coomassie Blue G250, 200 mM DTT), and appropriate volumes (5–20 μL) were loaded for two-layer Phos-tag PAGE as described above.

Supplemental Data

The following supplemental materials are available.

Supplemental Figure S1. Phosphatase treatment enhances detection of the phosphorylated form of Lhcb2.

Supplemental Figure S2. Specificity of the Lhcb1 and Lhcb2 antibodies against recombinant proteins.

Supplemental Figure S3. Determination of the linear range of the immunoblot assay.

Supplemental Figure S4. Phosphorylated and nonphosphorylated Lhcb1 or Lhcb2 are detected with similar efficiency.

Supplemental Figure S5. Phosphorylation kinetics in leaves of 6-week-old Arabidopsis plants.

Supplemental Figure S6. Evaluation of phosphorylation levels of Lhcb1 and Lhcb2 in the PSI-LHCII supercomplex.

Supplemental Figure S7. Quantification of Lhcb1 and Lhcb2 phosphorylation in PSII-LHCII supercomplexes.

LITERATURE CITED

Alboresi A, Caffarri S, Nogue F, Bassi R, Morosinotto T (2008) In silico and biochemical analysis of Physcomitrella patens photosynthetic antenna: identification of subunits which evolved upon land adaptation. PLoS One **3:** e2033

Allen JF (1992) Protein phosphorylation in regulation of photosynthesis. Biochim Biophys Acta **1098:** 275–335

Arnold J, Shapiguzov A, Fucile G, Rochaix JD, Goldschmidt-Clermont M, Eichacker LA (2014) Separation of membrane protein complexes by native LDS-PAGE. Plant Proteomics **1072:** 667–676

Bekešová S, Komis G, Křenek P, Vyplelová P, Ovečka M, Luptovčiak I, Illés P, Kuchařová A, Šamaj J (2015) Monitoring protein phosphorylation by acrylamide pendant Phos-Tag™ in various plants. Front Plant Sci **6:** 336

Bellafiore S, Barneche F, Peltier G, Rochaix JD (2005) State transitions and light adaptation require chloroplast thylakoid protein kinase STN7. Nature **433:** 892–895

Boekema EJ, Van Roon H, Van Breemen JFL, Dekker JP (1999) Supramolecular organization of photosystem II and its light-harvesting antenna in partially solubilized photosystem II membranes. Eur J Biochem **266:** 444–452

Caffarri S, Kouřil R, Kereïche S, Boekema EJ, Croce R (2009) Functional architecture of higher plant photosystem II supercomplexes. EMBO J **28:** 3052–3063

Croce R, van Amerongen H (2014) Natural strategies for photosynthetic light harvesting. Nat Chem Biol **10:** 492–501

Damkjaer JT, Kereïche S, Johnson MP, Kovacs L, Kiss AZ, Boekema EJ, Ruban AV, Horton P, Jansson S (2009) The photosystem II light-harvesting protein Lhcb3 affects the macrostructure of photosystem II and the rate of state transitions in *Arabidopsis*. Plant Cell **21:** 3245–3256

de Bianchi S, Dall'Osto L, Tognon G, Morosinotto T, Bassi R (2008) Minor antenna proteins CP24 and CP26 affect the interactions between photosystem II subunits and the electron transport rate in grana membranes of *Arabidopsis*. Plant Cell **20:** 1012–1028

Dietzel L, Bräutigam K, Steiner S, Schüffler K, Lepetit B, Grimm B, Schöttler MA, Pfannschmidt T (2011) Photosystem II supercomplex remodeling serves as an entry mechanism for state transitions in *Arabidopsis*. Plant Cell **23:** 2964–2977

Duffy CDP, Valkunas L, Ruban AV (2013) Light-harvesting processes in the dynamic photosynthetic antenna. Phys Chem Chem Phys **15:** 18752–18770

Formaggio E, Cinque G, Bassi R (2001) Functional architecture of the major light-harvesting complex from higher plants. J Mol Biol **314:** 1157–1166

Frenkel M, Bellafiore S, Rochaix JD, Jansson S (2007) Hierarchy amongst photosynthetic acclimation responses for plant fitness. Physiol Plant **129:** 455–459

Fristedt R, Herdean A, Blaby-Haas CE, Mamedov F, Merchant SS, Last RL, Lundin B (2015) PHOTOSYSTEM II PROTEIN33, a protein conserved in the plastid lineage, is associated with the chloroplast thylakoid membrane and provides stability to photosystem II supercomplexes in Arabidopsis. Plant Physiol **167:** 481–492

Galka P, Santabarbara S, Khuong TTH, Degand H, Morsomme P, Jennings RC, Boekema EJ, Caffarri S (2012) Functional analyses of the plant photosystem I-light-harvesting complex II supercomplex reveal that light-harvesting complex II loosely bound to photosystem II is a very efficient antenna for photosystem I in state II. Plant Cell **24:** 2963–2978

Goldschmidt-Clermont M, Bassi R (2015) Sharing light between two photosystems: mechanism of state transitions. Curr Opin Plant Biol **25:** 71–78

Grieco M, Suorsa M, Jajoo A, Tikkanen M, Aro EM (2015) Light-harvesting II antenna trimers connect energetically the entire photosynthetic machinery - including both photosystems II and I. Biochim Biophys Acta **1847:** 607–619

Haldrup A, Jensen PE, Lunde C, Scheller HV (2001) Balance of power: a view of the mechanism of photosynthetic state transitions. Trends Plant Sci **6:** 301–305

Jackowski G, Kacprzak K, Jansson S (2001) Identification of Lhcb1/Lhcb2/Lhcb3 heterotrimers of the main light-harvesting chlorophyll a/b-protein complex of Photosystem II (LHC II). Biochim Biophys Acta **1504:** 340–345

Jansson S, Selstam E, Gustafsson P (1990) The rapidly phosphorylated 25 kDa polypeptide of the light- harvesting complex of photosystem II is encoded by the type 2 cab-II genes. Biochim Biophys Acta **1019:** 110–114

Järvi S, Suorsa M, Paakkarinen V, Aro EM (2011) Optimized native gel systems for separation of thylakoid protein complexes: novel super- and mega-complexes. Biochem J **439:** 207–214

Kim E, Ahn TK, Kumazaki S (2015) Changes in antenna sizes of photosystems during state transitions in granal and stroma-exposed thylakoid membrane of intact chloroplasts in Arabidopsis mesophyll protoplasts. Plant Cell Physiol **56:** 759–768

Kinoshita E, Kinoshita-Kikuta E, Koike T (2009) Separation and detection of large phosphoproteins using Phos-tag SDS-PAGE. Nat Protoc **4:** 1513–1521

Kirchhoff H (2014) Structural changes of the thylakoid membrane network induced by high light stress in plant chloroplasts. Philos Trans R Soc Lond B Biol Sci **369:** 20130225

Kouřil R, Dekker JP, Boekema EJ (2012) Supramolecular organization of photosystem II in green plants. Biochim Biophys Acta **1817:** 2–12

Kouřil R, Zygadlo A, Arteni AA, de Wit CD, Dekker JP, Jensen PE, Scheller HV, Boekema EJ (2005a) Structural characterization of a complex of photosystem I and light-harvesting complex II of Arabidopsis thaliana. Biochemistry **44:** 10935–10940

Larsson UK, Sundby C, Andersson B (1987) Characterization of two different subpopulations of spinach light-harvesting chlorophyll a/b-protein complex (LHC II): Polypeptide composition, phosphorylation pattern and association with Photosystem II. Biochim Biophys Acta BBABioenerg **894:** 59–68

Leoni C, Pietrzykowska M, Kiss AZ, Suorsa M, Ceci LR, Aro EM, Jansson S (2013) Very rapid phosphorylation kinetics suggest a unique role for Lhcb2 during state transitions in Arabidopsis. Plant J **76:** 236–246

Mekala NR, Suorsa M, Rantala M, Aro EM, Tikkanen M (2015) Plants actively avoid state transitions upon changes in light intensity: role of light-harvesting complex II protein dephosphorylation in high light. Plant Physiol **168:** 721–734

Pagliano C, Nield J, Marsano F, Pape T, Barera S, Saracco G, Barber J (2014) Proteomic characterization and three-dimensional electron microscopy study of PSII-LHCII supercomplexes from higher plants. Biochim Biophys Acta **1837:** 1454–1462

Pietrzykowska M, Suorsa M, Semchonok DA, Tikkanen M, Boekema EJ, Aro EM, Jansson S (2014) The light-harvesting chlorophyll *a/b* binding proteins Lhcb1 and Lhcb2 play complementary roles during state transitions in Arabidopsis. Plant Cell **26:** 3646–3660

Pribil M, Pesaresi P, Hertle A, Barbato R, Leister D (2010) Role of plastid protein phosphatase TAP38 in LHCII dephosphorylation and thylakoid electron flow. PLoS Biol **8:** e1000288

Rochaix J-D (2014) Regulation and dynamics of the light-harvesting system. Annu Rev Plant Biol **65:** 287–309

Samol I, Shapiguzov A, Ingelsson B, Fucile G, Crèvecoeur M, Vener AV, Rochaix JD, Goldschmidt-Clermont M (2012) Identification of a photosystem II phosphatase involved in light acclimation in *Arabidopsis*. Plant Cell **24:** 2596–2609

Schägger H, von Jagow G (1991) Blue native electrophoresis for isolation of membrane protein complexes in enzymatically active form. Anal Biochem **199:** 223–231

Shapiguzov A, Ingelsson B, Samol I, Andres C, Kessler F, Rochaix JD, Vener AV, Goldschmidt-Clermont M (2010) The PPH1 phosphatase is specifically involved in LHCII dephosphorylation and state transitions in Arabidopsis. Proc Natl Acad Sci USA **107:** 4782–4787

Standfuss J, Kühlbrandt W (2004) The three isoforms of the light-harvesting complex II: spectroscopic features, trimer formation, and functional roles. J Biol Chem **279:** 36884–36891

Wientjes E, Drop B, Kouřil R, Boekema EJ, Croce R (2013a) During state 1 to state 2 transition in Arabidopsis thaliana, the photosystem II supercomplex gets phosphorylated but does not disassemble. J Biol Chem **288:** 32821–32826

Wientjes E, van Amerongen H, Croce R (2013b) Quantum yield of charge separation in photosystem II: functional effect of changes in the antenna size upon light acclimation. J Phys Chem B **117:** 11200–11208

Yokono M, Takabayashi A, Akimoto S, Tanaka A (2015) A megacomplex composed of both photosystem reaction centres in higher plants. Nat Commun **6:** 6675

Zer H, Vink M, Shochat S, Herrmann RG, Andersson B, Ohad I (2003) Light affects the accessibility of the thylakoid light harvesting complex II (LHCII) phosphorylation site to the membrane protein kinase(s). Biochemistry **42:** 728–738

Zhang Y, Liu C, Liu S, Shen Y, Kuang T, Yang C (2008) Structural stability and properties of three isoforms of the major light-harvesting chlorophyll a/b complexes of photosystem II. Biochim Biophys Acta **1777:** 479–487